MOLECULAR ECOLOGY

Molecular Ecology (2011) **20**, 2662–2675 doi: 10.1111/j.1365-294X.2011.05126.x

Genetic structuring and recent demographic history of red pandas (*Ailurus fulgens*) inferred from microsatellite and mitochondrial DNA

YIBO HU,*[1] YU GUO,*[1] DUNWU QI,* XIANGJIANG ZHAN,* HUA WU,* MICHAEL W. BRUFORD† and FUWEN WEI*

**Key Laboratory of Animal Ecology and Conservation Biology, Institute of Zoology, Chinese Academy of Sciences, 1-5 Beichen West Road, Beijing 100101, China, †Organisms and Environment Division, Cardiff School of Biosciences, Cardiff University, Cardiff CF10 3AX, UK*

Abstract

Clarification of the genetic structure and population history of a species can shed light on the impacts of landscapes, historical climate change and contemporary human activities and thus enables evidence-based conservation decisions for endangered organisms. The red panda (*Ailurus fulgens*) is an endangered species distributing at the edge of the Qinghai-Tibetan Plateau and is currently subject to habitat loss, fragmentation and population decline, thus representing a good model to test the influences of the above-mentioned factors on a plateau edge species. We combined nine microsatellite loci and 551 bp of mitochondrial control region (mtDNA CR) to explore the genetic structure and demographic history of this species. A total of 123 individuals were sampled from 23 locations across five populations. High levels of genetic variation were identified for both mtDNA and microsatellites. Phylogeographic analyses indicated little geographic structure, suggesting historically wide gene flow. However, microsatellite-based Bayesian clustering clearly identified three groups (Qionglai-Liangshan, Xiaoxiangling and Gaoligong-Tibet). A significant isolation-by-distance pattern was detected only after removing Xiaoxiangling. For mtDNA data, there was no statistical support for a historical population expansion or contraction for the whole sample or any population except Xiaoxiangling where a signal of contraction was detected. However, Bayesian simulations of population history using microsatellite data did pinpoint population declines for Qionglai, Xiaoxiangling and Gaoligong, demonstrating significant influences of human activity on demography. The unique history of the Xiaoxiangling population plays a critical role in shaping the genetic structure of this species, and large-scale habitat loss and fragmentation is hampering gene flow among populations. The implications of our findings for the biogeography of the Qinghai-Tibetan Plateau, subspecies classification and conservation of red pandas are discussed.

Keywords: *Ailurus fulgens*, demographic history, genetic structure, human activity, microsatellite, mitochondrial DNA

Received 27 January 2011; revision received 26 March 2011; accepted 6 April 2011

Introduction

The Qinghai-Tibetan Plateau and its neighbouring areas are global biodiversity hotspots (Myers *et al.* 2000) and a focal region for ecologists and conservation biologists. Historically, the uplift of the Qinghai-Tibetan Plateau has shaped extensive topographic variation in this region, with high mountains and large rivers. Landscape features and/or historical climate oscillations resulting from the Quaternary ice age have shaped the genetic structure and population history of wildlife in this region

Correspondence: Fuwen Wei, Fax: +86 10 64807099, E-mail: weifw@ioz.ac.cn

[1]These authors contributed equally to this work.

(Liu *et al.* 2007; Qu *et al.* 2010) which is now increasingly being affected by human activities (Zhang *et al.* 2007; Liu *et al.* 2009). The findings of previous phylogeographic research in this region have varied depending on the species, geographical context and life history traits such as dispersal ability. For instance, comparative phylogeography has shown that species or populations inhabiting the plateau platform underwent population expansions typically occurring after glaciation events but species or populations along the plateau edge have been shown to be relatively stable (e.g., Hu *et al.* 2010; Qu *et al.* 2010), although some studies have demonstrated that species or populations along the plateau edge also experienced population expansion (e.g., Liu *et al.* 2007; Sakka *et al.* 2010). However, the composite impact of landscapes, historical climate change and contemporary human activities on the genetic structure and population history of species remains poorly understood, because of very limited research on the fauna in this region (An *et al.* 2009; Qu & Lei 2009; Qu *et al.* 2010; Sakka *et al.* 2010), especially for middle-to-large-sized mammals (Zhang & Jiang 2006; Zhang *et al.* 2007; Liu *et al.* 2009).

The red panda (*Ailurus fulgens*) is a forest-dwelling endangered species distributed at the edge of the Qinghai-Tibetan Plateau that receives much interest because of its conservation status and specialized feeding biology (Glatston 1994). Red pandas were once widely distributed across Eurasia (Roberts & Gittleman 1984) but are now restricted to south Asia (Nepal, Bhutan, India and Myanmar) and China (Tibet, Sichuan and Yunnan provinces). In China, red pandas are mainly distributed on the eastern edge of the Qinghai-Tibetan Plateau spanning a wide range of elevation from the Qinghai-Tibetan Plateau to the western edge of the Sichuan Basin. Their range encompasses the Three Parallel Rivers of Yunnan Protected Area (Nujiang, Lancangjiang and Jinshajiang) and other large rivers such as the Dadu and Yalongjiang, which may affect spatial distribution of genetic variation in this species. Furthermore, red pandas have experienced an estimated population decline of as much as 40% in China as a consequence of habitat loss and fragmentation and poaching (e.g., Wei *et al.* 1999), but any genetic impact of increased human activities remains unclear, including whether the decline resulted in a genetic signature of population bottleneck and the exact magnitude and timing of the decline. Therefore, as a medium-sized solitary mammal distributed on the plateau edge, red pandas represent a good model to understand the effects of landscapes, historical climatic oscillations and contemporary human activities on species' genetic structure and population history, which would contribute to the comprehensive understanding of the complex biogeography of the Qinghai-Tibetan Plateau.

Studies have attempted to use mitochondrial DNA markers (control region and/or cytochrome *b*) to investigate phylogeography and population history in red pandas but have found no obvious patterns (Su *et al.* 2001; Li *et al.* 2005). Su *et al.* (2001) sequenced a 236-bp fragment of mitochondrial DNA control region (mtDNA CR) in a sample size of 53 red pandas and detected no genetic divergence between the Sichuan and Yunnan populations. Li *et al.* (2005) amplified 551 bp of mtDNA CR and 398 bp of cytochrome *b* for 41 red pandas with the same result. However, combining microsatellite and mitochondrial DNA markers with contrasting modes of inheritance and rates of evolution can potentially provide a more accurate and comprehensive understanding of historical and recent evolutionary events (e.g., Heller *et al.* 2008; Ahonen *et al.* 2009; Urquhart *et al.* 2009), including in red pandas.

Here, using extensive field sampling, nine microsatellite loci and mtDNA CR sequences, we analysed genetic structure and population history of red pandas on the eastern edge of the Qinghai-Tibetan Plateau. Specifically, we aimed (i) to investigate the effects of landscape features, historical climatic changes and contemporary human activities on genetic structure and population history; and (ii) to elucidate patterns of demographic change and possible causes. Finally, we discuss the implications of our findings for the biogeography of the Qinghai-Tibetan Plateau, subspecies classification and conservation in this high-profile animal.

Materials and methods

Sample collection

Blood, muscle, skin, hair and faecal samples from wild red pandas were collected from nature reserves, zoos and museums across 23 geographical locations throughout their current distribution range (Fig. 1). Specifically, most samples of blood, muscle, skin and hair were obtained from zoos and museums and traced to their sources according to archival records, and most faecal samples were from the field (Table S1, Supporting Information). The faecal samples and all the other samples were confirmed as different individuals by microsatellite-based individual identification (e.g., Zhan *et al.* 2006) as shown later. As a result, 123 individuals were analysed comprising 14 blood samples, 11 muscle samples, 24 dried skins, 46 hair samples and 28 faecal samples (Table S1, Supporting Information). Most samples were located in four mountain ranges (defined here as populations): Qionglai (QL, $n = 31$), Liangshan (LS, $n = 39$) and Xiaoxiangling (XXL, $n = 27$) in Sichuan Province, and Gaoligong (GLG, $n = 22$) in Yunnan, including two samples from northern Myanmar. Four

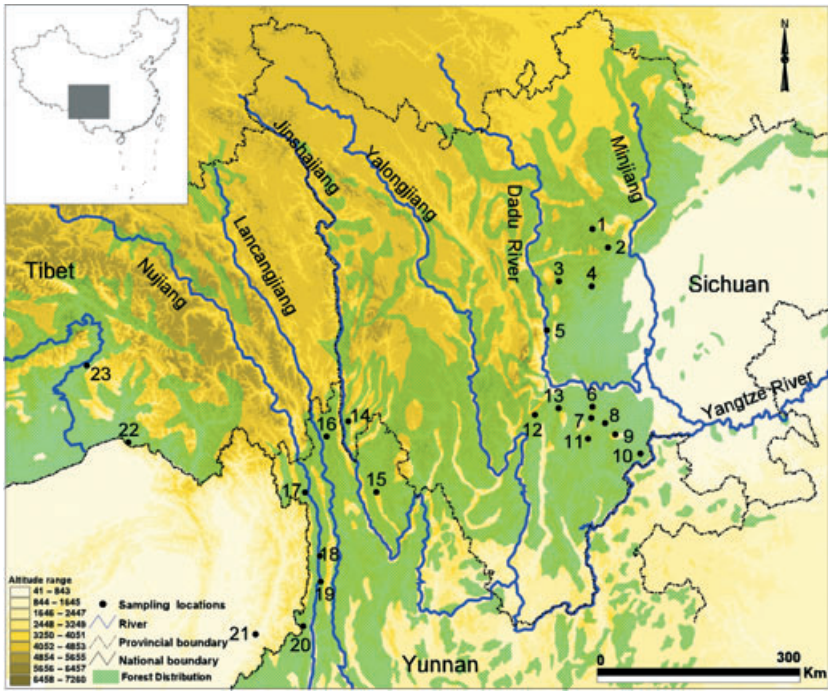

Fig. 1 Study area and sampling locations of red pandas across Tibet, Sichuan and Yunnan in China and northern Myanmar. Qionglai Mountains (QL): (1) Lixian, (2) Wenchuan, (3) Kangding, (4) Baoxing, (5) Luding. Liangshan Mountains (LS): (6) Ebian, (7) Ganluo, (8) Meigu, (9) Mabian, (10) Leibo, (11) Yuexi. Xiaoxiangling Mountains (XXL): (12) Mianning, (13) Shimian. Gaoligong Mountains (GLG): (14) Derong, (15) Zhongdian, (16) Deqin, (17) Gongshan, (18) Fugong, (19) Bijiang, (20) Lushui, (21) northern Myanmar. Tibet (TIB): (22) Nielamu, (23) Muotuo. The *inset* shows the location of the study area in China and northern Myanmar.

samples from Tibet were treated as a single population (TIB, $n = 4$). Because of a small sample size, the population TIB was removed from demographic analyses. The study area is divided by several large rivers (Fig. 1). Dadu River divides QL and XXL-LS; Yalongjiang divides XXL-LS and GLG; and the GLG population is further partitioned into four parts by the Nujiang, Lancangjiang and Jinshajiang Rivers.

Molecular analysis

Genomic DNA was extracted from blood, tissue and skin using the SDS–phenol/chloroform method (Sambrook *et al.* 1989), from plucked hair using the Chelex-100 method (Walsh *et al.* 1991) and from faeces following Zhang *et al.* (2006). Standard controls were used in extractions and downstream PCR amplifications.

Five hundred and fifty-one base pairs of mtDNA CR was amplified for each individual with the forward primer (5′-CACCATCAACACCCAAAGCTG-3′; Su *et al.* 2001) and the reverse (H16781, 5′-TTATGTCCTGTGACCATTGACTGA-3′; Li *et al.* 2005). Amplification was carried out in 20 μL containing 1–2 μL DNA, 10 μL Premix *Ex Taq* (TaKaRa), 0.4 μM forward and reverse primers and 0.5 μg/μL BSA (Sigma). PCR was performed as follows: initial denaturation at 94 °C for 5 min, followed by 35 cycles of PCR (94 °C/30 s, 54 °C/40 s, 72 °C/50 s) and a final step of 72 °C for 10 min. PCR products were purified and subsequently sequenced on an ABI 3100 DNA sequencer (Applied Biosystems).

Nine microsatellite loci—RP-11, RP-102, RP-137 and RP-219 (Liu *et al.* 2005), RP-108, RP-133, and RP-215 (redesigned), Aifu-1 and Aifu-23 (Liang *et al.* 2007)—were selected for this study (Table S2, Supporting Information) from 26 red panda-specific microsatellite loci. PCR was performed in 20 μL containing 1–2 μL DNA, 10 μL HotStarTaq Master Mix (Qiagen), 0.2 μM forward primer end-labelled with a fluorescent dye (HEX, FAM or TAMRA), 0.2 μM reverse primer and 0.5 μg/μL BSA (Sigma). The first step started with 94 °C for 15 min, followed by a touchdown PCR (a total of 35–40 cycles of 94 °C/30 s, T_m/40 s, 72 °C/50 s) and a final step of 72 °C for 15 min. T_m was decreased by 2 °C every second cycles from 60 °C to a final temperature of 48–50 °C, which was used for the next 25 cycles. Positive products were resolved on an ABI 3730 sequencer and scored using GeneScan 3.7 and Genotyper 3.7 (Applied Biosystems). To obtain reliable genotypes, amplification was repeated three times for DNA from blood, muscle and skin samples. For faecal and hair samples, a modified multi-tube approach (Taberlet *et al.* 1996; Zhan *et al.* 2006) was used to derive reliable

consensus genotypes. First, each extract was amplified twice simultaneously and loci that produced the same heterozygous genotype were accepted as heterozygous. Otherwise, a third repeat was performed and loci in which two alleles occurred at least twice were determined as heterozygous. If not, four additional positive reactions were conducted. Individual identification was performed for all the genotypes following Zhan *et al.* (2006). Among faecal and hair genotypes, the mean genotyping error rate per locus and overall error rate were computed (Zhan *et al.* 2010). For the final result of individual identification, Micro-Checker (Van Oosterhout *et al.* 2004) was utilized to detect the presence of null alleles and genotyping errors such as large allele dropout and stuttering.

MtDNA data analysis

MtDNA CR sequences were aligned using SeqManII in DNAStar (Burland 2000) and checked visually. Sequence comparison and measurement of variability were performed using MEGA 4.0 (Tamura *et al.* 2007), and unique haplotypes were identified using DAMBE (Xia & Xie 2001). Phylogenetic relationships among mtDNA haplotypes were estimated by maximum-likelihood (ML) analysis using PAUP*4.0 (Swofford 2002). The most likely DNA substitution model was selected using jModelTest v0.1 (Guindon & Gascuel 2003; Posada 2008). A median-joining network (Bandelt *et al.* 1999) based on maximum parsimony was also used to reconstruct the phylogenetic relationships among haplotypes using NETWORK 4.5.1.6 (http://www.fluxus-engineering.com).

Nucleotide diversity (π, Nei 1987) and haplotype diversity (h, Nei 1987) were estimated using DnaSP 5.0 (Librado & Rozas 2009). Genetic differentiation (F_{ST}) between populations was assessed based on haplotype frequency differences (Excoffier *et al.* 2005). Isolation-by-distance (IBD) pattern between Euclidean geographical distances and genetic distances (F_{ST}) was tested using the Mantel test (Mantel 1967). To explore possible influences of single population, IBD was also tested using a leave-one-out jackknifing method. Above-mentioned analyses were implemented in ARLEQUIN 3.5 (Excoffier *et al.* 2005) with 20 000 permutations. Significance values for multiple comparisons were adjusted using the Bonferroni correction (Rice 1989). To identify spatial pattern of genetic structure, spatial analysis of molecular variance (SAMOVA; Dupanloup *et al.* 2002) was used to detect groups of populations that maximize genetic differentiation each other (Φ_{CT}) and were statistically significant, with a range of k values from 2 to 4.

To test the hypothesis of demographic expansion, the population parameter $\theta = 2N_{ef}\mu$ (N_{ef} is the female effective population size and μ is the mutation rate per site per generation) was estimated using π (Tajima 1983) and θ_W [Watterson's (1975) point estimator] with DnaSP 5.0. The estimator π uses the recent population as the population of inference and θ_W uses the historical population as the population of inference. Furthermore, Tajima's D test (Tajima 1989) and Fu's F_s test (Fu 1997) were performed with ARLEQUIN 3.5 to detect a signal of population expansion as departure from neutrality could also be attributed to factors other than selective effects, such as demographic expansion or bottleneck (Ramos-Onsins & Rozas 2002). Finally, a coalescent-based method implemented in FLUCTUATE 1.4 (Kuhner *et al.* 1998) was used to estimate the ML estimate of θ for variable population sizes ($\theta_{g = var}$) and population growth parameter (g), which applies θ_W as a starting parameter and uses genealogical information in the data for Markov Chain Monte Carlo (MCMC) simulations.

Microsatellite data analysis

The mean number of allele (MNA) per locus and observed (H_O) and expected heterozygosities (H_E) were calculated using ARLEQUIN 3.5. Inbreeding coefficients (F_{IS}) were estimated with FSTAT 2.9.3.2 (Goudet 2001), which we also used to test linkage disequilibrium. To compare allele diversity between populations, ARES 1.2.3 (Van Loon *et al.* 2007) based on an extrapolation model was used to assess population's mean allelic richness (the number of alleles) with 95% confidence bounds, corrected for differences in sample size. Deviations from Hardy–Weinberg equilibrium across all loci for each population were assessed using an exact probability test implemented in GENEPOP 4.0 (Rousset 2008). Significance values for multiple comparisons were adjusted using the Bonferroni correction.

Genetic differentiation (F_{ST}) between populations was estimated and IBD was tested with the same analyses as mtDNA data, using ARLEQUIN 3.5. A Bayesian clustering method, STRUCTURE (Pritchard *et al.* 2000), was used to detect genetic clustering in the whole data set. Under STRUCTURE 2.2.3, the range of possible clusters (K) tested was set from 1 to 8, and 10 independent runs were carried out for each using no prior information, assumed admixture and correlated allele frequencies. The lengths of MCMC iteration and burn-in were set at 1 000 000 and 100 000, respectively. The true K is selected using the maximal value of the log likelihood [Ln Pr(X/K)] of the posterior probability of the data for a given K (Pritchard *et al.* 2000). Further, the ΔK statistic, the second-order rate of change in the log probability of the data between successive values of K, was also estimated (Evanno *et al.* 2005).

Recent migration rates among identified genetic clusters were assessed using a Bayesian MCMC analysis implemented in BAYESASS 1.3 (Wilson & Rannala 2003) which does not assume Hardy–Weinberg equilibrium within populations. We set delta values for allele frequencies (0.1), inbreeding coefficients (0.15) and immigration rates (0.15) so that acceptance rates for changes in these parameters fell between 40% and 60% (Wilson & Rannala 2003). The analysis was run three times with different random seeds to check for consistency of results; 6×10^6 iterations were used including a burn-in of 2×10^6.

Demographic history based on microsatellite was assessed using three different and complementary methods. First, a heterozygosity excess test (Cornuet & Luikart 1996) was performed under three microsatellite mutation models: infinite allele model (IAM), stepwise mutation model (SMM) and two-phase mutation model (TPM). Under the TPM, the proportion of one-step mutation was set as 90% or 95% and the variance as 12. The Wilcoxon signed-rank test was used to evaluate significance based on 10 000 repetitions. Second, a mode-shift test (Luikart *et al.* 1998) was carried out to detect a distortion of the expected L-shaped distribution of allele frequency. Both heterozygosity excess and mode-shift tests were implemented in BOTTLENECK 1.2.02 (Piry *et al.* 1999). Finally, a coalescent-based Bayesian method (Storz & Beaumont 2002) was used to infer population demographic change as implemented in MSVAR 1.3, which is based on the observed allele distribution and allele frequencies (e.g., Goossens *et al.* 2006). Wide priors and three independent runs were used, and variances for these prior distributions were large to affect posterior distributions as little as possible, as used in Hu *et al.* (2010). Different hyperprior means for the mean ancestral population size (N_1) were used to represent possible demographic histories (stable, decreased or increased). The total number of iterations was 1×10^9 or 1.5×10^9, and the thinning interval was 1×10^4 or 1.5×10^4. The first 10% of total iterations were discarded to avoid bias in parameter estimation, and the remaining data were used to obtain the lower (5%), median (50%) and upper (95%) quantiles of the posterior distributions. The generation time of wild red pandas is unavailable, but in captivity, the sexual maturity age of red pandas was 2 years old (Hu 1991) and the generation time estimated was approximately 4.5 years (Princée 1989). Here, a generation time of 4 years was used for independent MSVAR simulations, but 2 or 6 years were also utilized to assess possible influences of different generation times on simulation results.

Results

Genetic variations

Five hundred and fifty-one base pairs of mtDNA CR sequences were obtained from 119 individuals. Forty-three variable nucleotide sites were found, comprising 39 transitions, three transversions and one transition/transversion (Table S3, Supporting Information). Twenty-nine haplotypes were defined (Table S3, Supporting Information, 22 haplotypes deposited in GenBank under Accession Nos HQ992964–HQ992985), and seven were identical to those reported by Li *et al.* (2005): R1 (Hap28), R2 (Hap13), R5 (Hap14), R6 (Hap05), R11 (Hap01_3), R25 (Hap37) and R29 (Hap31). Ten haplotypes were shared between QL/LS (R2, R3, R4, R5, R7 and R9), QL/LS/XXL (R6, R11), QL/LS/XXL/GLG (R10) and LS/GLG (R12), respectively. While haplotypes R6, R10 and R11 occupied a wide geographic distribution, 19 of 29 haplotypes were restricted to one population (Table S4, Supporting Information). High haplotype diversity (0.924 ± 0.012) and relatively low nucleotide diversity (0.0158 ± 0.0005) were detected

Table 1 Genetic variations based on mitochondrial control region and nine microsatellite loci in five populations of red pandas

Population	*N* (CR/MS)	*H*	*h* ± SD	π ± SD	MNA	H_O	H_E	F_{IS}
QL	30/26	12	0.917 ± 0.025	0.0162 ± 0.0012	6.2	0.743	0.688	−0.083
LS	39/28	12	0.862 ± 0.029	0.0156 ± 0.0008	5.8	0.700	0.702	0.003*
XXL	26/27	4	0.643 ± 0.074	0.0121 ± 0.0008	5.8	0.564	0.634	0.113*
GLG	20/20	12	0.942 ± 0.029	0.0145 ± 0.0016	7.1	0.712	0.732	0.027
TIB†	4/4	3	0.833 ± 0.222	0.0163 ± 0.0048	4.6	0.722	0.770	0.071
Total	119/105	29	0.924 ± 0.012	0.0158 ± 0.0005	9.2	0.679	0.719	0.057*

N, number of individuals; CR, mitochondrial control region; MS, microsatellite; SD, standard deviation; *H*, haplotype number; *h*, haplotype diversity; π, nucleotide diversity; MNA, mean number of allele per locus; H_O and H_E, observed and expected heterozygosity; F_{IS}, inbreeding coefficient.

*Deviation from Hardy–Weinberg equilibrium ($P < 0.01$).

†the genetic variation of TIB was not discussed in the text due to a small sample size.

for the whole populations. Among the five populations, XXL possessed the lowest haplotype diversity and nucleotide diversity, but QL, LS and GLG had similar levels of mtDNA diversity (Table 1).

For microsatellites, 105 individuals were successfully genotyped (more than six loci), of which 78 individuals had nine loci, 17 individuals had eight loci, eight individuals had seven loci and only two individuals had six loci. For the faecal and hair genotypes, the mean genotyping error rate per locus was 1.94×10^{-7} and the overall error rate across 9 loci was 1.75×10^{-6}. For the final data set of 105 individuals, Micro-Checker detected no evidence of null alleles or genotyping errors such as large allele dropout and stuttering. The mean number of alleles per locus (MNA) ranged between 4.6 and 7.1, and average H_E and H_O values were 0.634–0.770 and 0.564–0.743, respectively. XXL had the lowest H_E and H_O, and GLG have the highest MNA and H_E among these populations excluding TIB (Table 1), but ARES showed that after extrapolating beyond the sample sizes, the allelic richness of GLG is similar to QL and LS and statistically insignificant (Fig. S1, Supporting Information). Test of Hardy–Weinberg equilibrium showed that the XXL and LS populations deviated from equilibrium (Table 1). The test for linkage disequilibrium demonstrated that no linkage disequilibrium occurred for any pair of loci in any population (after the Bonferroni correction).

Phylogeography and population genetic structure

Hierarchical likelihood ratio tests indicated a HKY model of substitution with heterogeneity and gamma distribution as the best fit for the mtDNA CR data (HKY + I + G; $-\ln L = 1183.8136$; Ti/Tv ratio = 1109.9017; gamma distribution shape = 0.327; base frequencies of A = 0.2715, C = 0.248, G = 0.1693 and T = 0.3112). The unrooted ML tree for CR haplotypes showed that clusters with higher bootstrap support were either from the same sampling location or from different geographic populations, thus indicating only localized but no broad geographic structure (Fig. S2, Supporting Information). The median-joining network produced a complex pattern with no obvious phylogeographic structure (Fig. 2). Although 19 haplotypes were unique to a single population, the network showed little evidence for overt phylogeographic structure. The SAMOVA analysis found that the population grouping with the highest Φ_{CT} value (0.102) was QL-LS-XXL and GLG-TIB ($k = 2$) but was not statistically supported ($P = 0.095$), and only 10.2% of the genetic variation was explained by variation among groups whereas variation within populations accounted for 86.4% of the total variation. For $k = 3$, the final genetic structure was QL-LS-XXL,

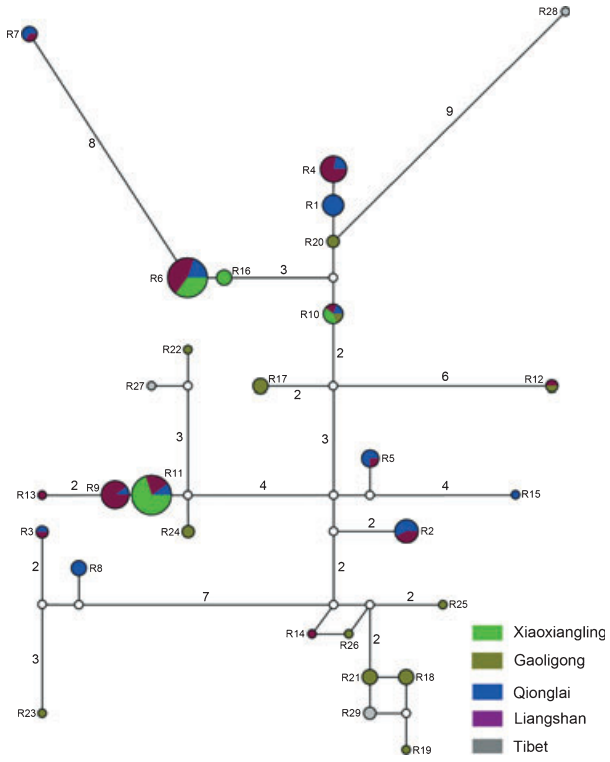

Fig. 2 Median-joining network based on maximum parsimony among mtDNA CR haplotypes of red pandas. *Nodes* contain the haplotype name and are proportional to haplotype frequencies. Length of *branches* is proportional to the number of changes from one haplotype to the following, with a number next to the branch representing more than one mutation step. *Empty nodes* indicate undetected intermediate haplotype states.

GLG and TIB ($\Phi_{CT} = 0.09$, $P = 0.102$), also indicating no significant population groups.

For mtDNA and microsatellite data, F_{ST} analyses produced similar results: significant F_{ST} values were detected between populations except for QL vs. LS (Table 2) (Most of F_{ST} estimates between TIB and other populations were large but insignificant possibly because of a small sample size). IBD tests detected no significant correlation between geographical distances and F_{ST} values for the whole sample, regardless of mtDNA or microsatellite data (Table 3). In addition, we performed a transformation for geographical distance [namely Ln (geographical distance)] and for F_{ST} [namely $F_{ST}/(1 - F_{ST})$], respectively, and also found no significant correlation (data not shown). Interestingly, a significant IBD pattern was detected after removing the XXL population based on microsatellite ($r = 0.861$, $P = 0.043$; Table 3), and for mtDNA data, there was a similar pattern but with no statistical support ($r = 0.732$, $P = 0.081$).

STRUCTURE analysis revealed a maximum log likelihood of posterior probability of the genetic data at $K = 3$ [Ln

Table 2 Pairwise F_{ST} estimates based on mtDNA control region and microsatellite data, respectively

Population	QL	LS	XXL	GLG	TIB
QL		0.0081	0.0964***	0.0529***	0.1235***
LS	0.04		0.0586***	0.0287*	0.0796*
XXL	0.1548***	0.1403***		0.0839***	0.0676
GLG	0.0692***	0.0977***	0.2101***		0.0252
TIB	0.1126	0.1475	0.2987*	0.0981	

Above diagonal: pairwise F_{ST} values based on microsatellite data; below diagonal: pairwise F_{ST} values based on mtDNA CR data. The significance was indicated after the Bonferroni correction: *P < 0.005, **P < 0.001 and ***P < 0.0001.

Table 3 Results of the Mantel tests analysing the correlation between Euclidean geographical distances and genetic distances (F_{ST}) based on microsatellite data

	All	XXL*	QL*	LS*	GLG*	TIB*
Correlation coefficient (r)	0.338	0.861	0.188	0.082	0.528	−0.076
Significance (P)	0.178	0.043	0.417	0.424	0.121	0.541
Determination ratio	0.114	0.741	0.035	0.007	0.279	0.006

All, a Mantel test for the whole sample; Population with an asterisk (*), a Mantel test after removing this population; Determination ratio, the percent of genetic variations explained by geographical distance.

$P(X/K)$ = −2824.63]. Moreover, the ΔK value based on the STRUCTURE output also showed a clear maximum (ΔK = 123.57) at K = 3 (Fig. 3a). These results showed a strong genetic structuring among populations, largely following the mountain-range origins of each individual, but with some misassignment (Fig. 3b). Individuals from GLG and TIB predominantly formed a separate cluster, being clearly differentiated with QL and XXL. Individuals from QL formed a cluster together with most individuals from LS, and individuals from XXL formed a single cluster along with some individuals from LS. The assignment result for LS individuals implied obvious gene flow between LS and its adjacent populations. Among the three genetic clusters, recent migration rate estimation indicated that migration rates were relatively low, ranging from 0.004 to 0.084 (Table 4).

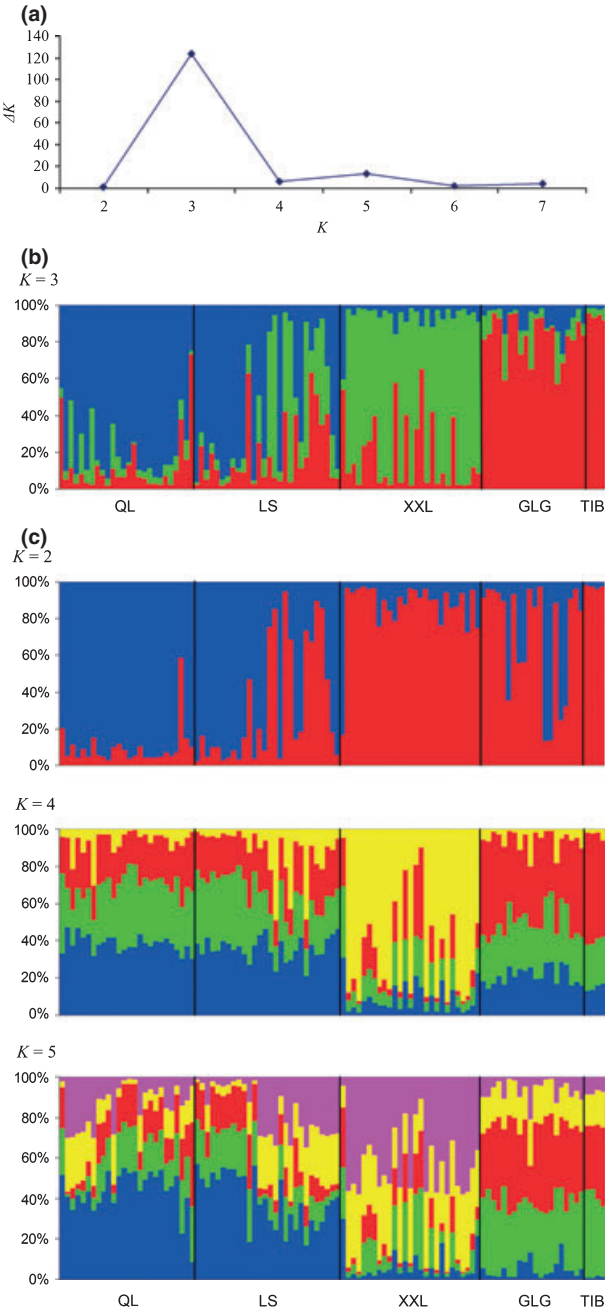

Fig. 3 Bayesian STRUCTURE clustering results based on microsatellite genotypes among five red panda populations. (a) ΔK values as a function of K based on 10 runs, indicating the most likely number of three genetic clusters, (b) STRUCTURE output of three genetic clusters identified (K = 3), represented by three colours: blue, green and red. The proportions of ancestry assigned to different clusters were plotted by individuals, (c) STRUCTURE assignment outputs at K = 2, 4 and 5.

Demographic history

Based on mtDNA CR data, the point estimators π and θ_W were similar for the whole sample and any population except for XXL, indicating no significant support for population expansion. Tajima's D test, Fu's F_s test, population growth parameter (g) and historical female effective population size ($\theta_{g\ =\ var}$) also suggested the same pattern (Table 5), although GLG demonstrated

Table 4 Migration rates between three genetic clusters based on microsatellite data, with 95% confidence intervals in the brackets

	To QL-LS	To XXL	To GLG-TIB
From QL-LS	**0.99** (0.965–1.00)	0.05 (0.007–0.11)	0.068 (0.003–0.162)
From XXL	0.006 (0.00004–0.027)	**0.93** (0.866–0.977)	0.084 (0.002–0.245)
From GLG-TIB	0.004 (0.00004–0.017)	0.02 (0.0006–0.063)	**0.848** (0.735–0.944)

Non-migration rate in each genetic cluster is marked in bold.

Table 5 Estimates of population demographic parameters based on mtDNA control region data

Population	$\pi \pm$ SD	$\theta_W \pm$ SD	$\theta_{g=var} \pm$ SD	$g \pm$ SD	D (P-value)	F_s (P-value)
QL	0.0162 ± 0.0012	0.0137 ± 0.0025	0.027 ± 0.004	42.3 ± 36.4	0.645 (0.797)	1.346 (0.716)
LS	0.0156 ± 0.0008	0.0142 ± 0.0025	0.026 ± 0.004	19.3 ± 34.9	0.357 (0.703)	2.307 (0.825)
XXL	0.0121 ± 0.0008	0.0067 ± 0.0018	0.003 ± 0.001	−190.6 ± 81.5	2.830 (0.999)	8.808 (0.997)
GLG	0.0145 ± 0.0016	0.0169 ± 0.0029	0.048 ± 0.009	125.4 ± 38.1	−0.565 (0.302)	−0.896 (0.354)
Total	0.0158 ± 0.0005	0.0146 ± 0.0022	0.039 ± 0.004	38.0 ± 30.4	0.264 (0.666)	−1.994 (0.325)

The population parameter θ was estimated using Watterson's (1975) θ_W, and Kuhner *et al.*'s (1998) $\theta_{g=var}$ which allows for population change. For direct comparison, nucleotide diversity (π) was reported here again. g, population growth parameter; D, Tajima's D test value; F_s, Fu's F_s test value; SD, standard deviation.

relatively larger g and $\theta_{g=var}$ than QL and LS. However, Tajima's D test, Fu's F_s test, g and $\theta_{g=var}$ indicated a historical population contraction for XXL (Table 5).

BOTTLENECK tests based on microsatellite did not provide strong evidence for a recent bottleneck for any population or genetic cluster. The heterozygosity excess test found no significant excess under either SMM or TPM (regardless of the proportion of single-step mutations). However, significant excess occurred under the IAM, a less appropriate model for microsatellite than the SMM (Shriver *et al.* 1993). Hence, we considered the result based on the IAM as invalid. The mode-shift test showed a normal L-shape distribution of allele frequencies in any population. However, Bayesian MSVAR simulations revealed that QL and XXL have experienced recent and rapid population declines, and GLG demonstrated a pattern of relatively slow population decrease (Table 6, Fig. 4). The simulations using different generation times gave similar results (Tables 6 and S5, Supporting Information). For QL and XXL, the median current (N_0) and ancestral (N_1) effective population sizes were 343 and 18 839, and 228 and 14 939, respectively, both showing population declines in the order of 98% starting from 1750 or 1100 years ago (Fig. 4a,b). The median N_0 and N_1 of the GLG population were 2588 and 15 522, equivalent to a population decline of 83% commencing 10 747 years before present (Fig. 4c). Because the population LS had much gene flow with the adjacent populations and thus violated the assumption of population closure, we did not perform MSVAR simulation for this population.

Discussion

High genetic diversity

Because of massive habitat loss, increased human activities and poaching, red pandas have undergone population decline (e.g., Wei *et al.* 1999). Total population size in China is estimated at approximately 6400–7600, including 3000–3400 in Sichuan, 2000–2600 in Yunnan and 1400–1600 in Tibet (Wei *et al.* 1999; Hu & Du 2002). However, our assessment of genetic variations based on mtDNA and microsatellites indicated high levels of genetic diversity in this species. For the whole popula-

Table 6 Medians of current (N_0) and ancestral effective population sizes (N_1) and time since population decline (T) for the QL, XXL and GLG populations based on a generation time of 4 years, using Bayesian MSVAR simulations

Population	$N_0 \pm$ SD	$N_1 \pm$ SD	T (years) ± SD
QL	343 ± 39(5–5031)	18 839 ± 570 (2416–150 964)	1750 ± 515 (20–38 973)
XXL	228 ± 46 (1–5624)	14 939 ± 1076 (1800–141 559)	1100 ± 208 (4–91 288)
GLG	2588 ± 475 (19–1 041 700)	15 522 ± 832 (738–997 064)	10 747 ± 1269 (1–142 960 000)

Standard deviation (SD) was computed across three repeated runs, and values in the bracket were the 0.05 and 0.95 quantiles.

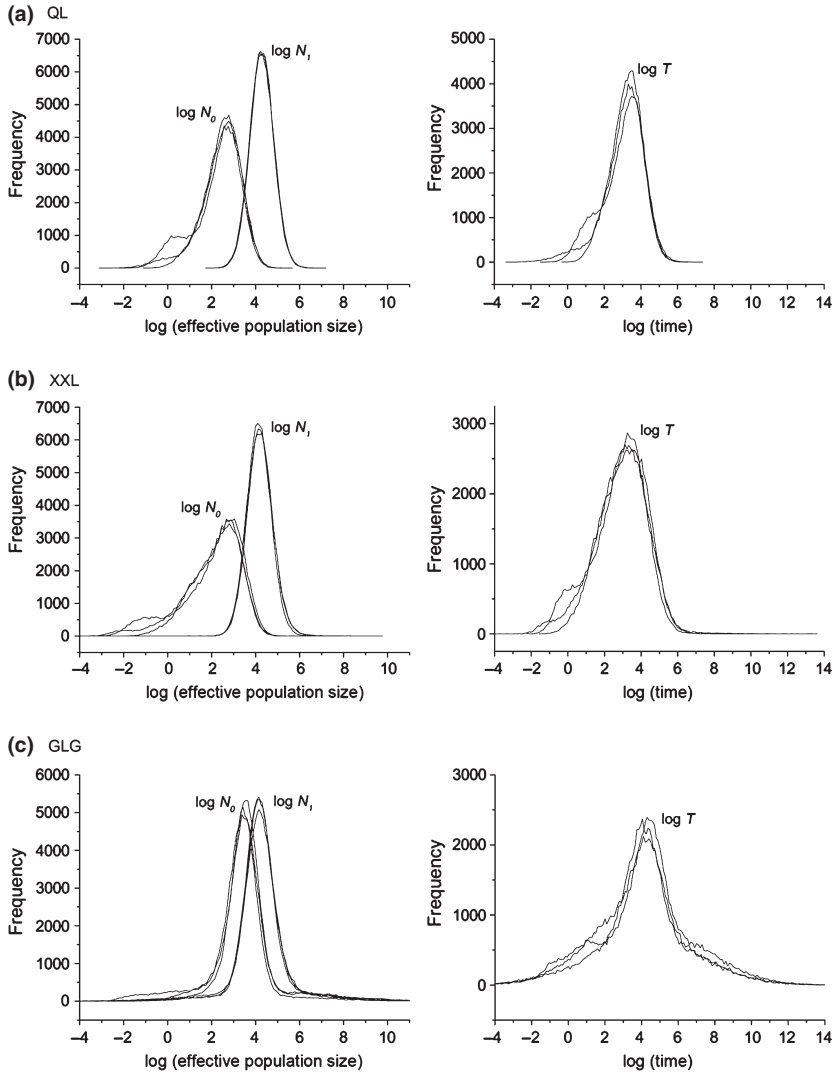

Fig. 4 Posterior distributions of current (N_0) and ancestral (N_1) effective population sizes and time since population change (T) on a logarithmic scale based on a generation time of 4 years from MSVAR simulations of three populations (a) QL, (b) XXL and (c) GLG.

tions, mtDNA CR haplotype diversity (h = 0.924) is similar to the findings of Li *et al.* (2005) (h = 0.95) and Su *et al.* (2001) (h = 0.93). High microsatellite diversity was also detected with the MNA and H_E being 9.2 and 0.719, respectively. At the species level, the microsatellite diversity in red pandas is slightly higher than or similar to those of other endangered carnivore species such as giant pandas (*Ailuropoda melanoleuca*, MNA = 7.1 and H_E = 0.642; Zhang *et al.* 2007), polar bears (*Ursus maritimus*, MNA = 6.5 and H_E = 0.68; Paetkau *et al.* 1999) and jaguars (*Panthera onca*, MNA = 8.3 and H_E = 0.739; Eizirik *et al.* 2001). These results suggest that despite a trend of population decline, high genetic variation has been maintained in wild populations, perhaps because of a large effective population size.

Genetic structure and population history

Despite more and wider sampling locations, phylogenetic tree and network analyses of mtDNA revealed no obvious geographic structure for red pandas, suggesting historically wide gene flow. SAMOVA also did not detect significant genetic structuring among populations. This finding is consistent with the results of Su *et al.* (2001) and Li *et al.* (2005) and is similar to other edge species in the Qinghai-Tibetan Plateau (e.g., Zhang *et al.* 2007; Qu *et al.* 2010). Historically, red pandas were likely only marginally affected by the Quaternary glaciations in the Qinghai-Tibetan Plateau, and thus they were not restricted to several refugia-like sites. As a result, gene flow could occur widely and obvious phylogeographic structure did not form. This inference was strengthened

by the population history of red pandas. The mtDNA-based demography did not support the hypothesis of population expansion or contraction for the whole sample or any population except for XXL, indicating relatively stable demography and less effects of the Quaternary glaciations. With larger sample size (119 individuals) and more sampling locations (23 locations), our finding was different from that of Li *et al.* (2005) (41 individuals from 11 locations) and Su *et al.* (2001) (53 individuals from eight locations), but is consistent with the demography of other species that inhabit the plateau edge such as giant pandas (Hu *et al.* 2010), twites (*Carduelis flavirostris*) and black redstarts (*Phoenicurus ochruros*) (Qu *et al.* 2010). Surprisingly, the result for XXL suggests a complex population history. Tajima's *D* test, Fu's F_s test and *g* showed an obvious signal of population contraction. But the comparison of the historical population parameters θ_W (0.0067) and $\theta_{g = var}$ (0.003) with the current population parameter π (0.0121) implied a population growth after the historical contraction.

With a different pattern of inheritance and rate of evolution from mtDNA, however, microsatellite-based analyses indeed detected significant genetic structure among populations. The evidences are clear: (i) STRUCTURE revealed three genetic clusters, i.e., QL-LS, XXL and GLG-TIB; and (ii) F_{ST} values between populations were significant except for QL vs. LS. Furthermore, genetic divergence was also reflected by mtDNA-based F_{ST} estimates. Although the Mantel test detected no IBD pattern for the whole sample, significant IBD occurred after removing XXL, indicating that geographical distance may work in shaping genetic structure of this species, but the XXL population obscured the IBD pattern. Across the study area, large rivers are a kind of dominant landscape feature and we hypothesized they would affect gene flow. Based on the Bayesian clustering results, however, the hypothesis was rejected. Both XXL and LS are located in the south of the Dadu River and are separated from QL by the river. Unexpectedly, significant differentiation occurred only between QL and XXL, but not between QL and LS. Moreover, there was genetic divergence between XXL and LS where no large rivers exist. The most likely explanation for this pattern is that the unique population history of XXL affected the whole genetic structure of red pandas (Table 5). Historically, the XXL population experienced population contraction, resulting in increased genetic drift and inbreeding and loss of genetic diversity. As a consequence, genetic divergence occurred between XXL and the adjacent populations QL, LS and GLG. Although XXL might have recovered after the historical contraction, divergence between XXL and the adjacent populations could not be diminished because of the isolation of wide unsuitable habitat gap between populations resulting from anthropogenic habitat loss and fragmentation. In our study area, alongside of human settlements along rivers, deforestation, reclamation and road construction rapidly eroded the habitat of red pandas. Consequently, wide unsuitable habitat gap between populations formed and hampered gene flow of this species to some extent. This inference that the uniqueness of XXL played a critical role in forming whole genetic structure was further supported by three pieces of evidence. First, the lowest genetic diversity was identified for XXL regardless of the measure of mtDNA or microsatellite (Table 1). Second, significant F_{IS} indicated some extent of inbreeding in the XXL population (Table 1). Finally, the uniqueness of XXL obscured the IBD pattern (Table 3). In contrast, historically LS experienced relatively stable population demography and maintained some level of gene flow with the adjacent QL which had similar demographic history to LS (Table 5). Thus, no significant divergence formed between the populations. Although anthropogenic habitat loss and fragmentation also occurred between LS and QL, the differentiation was difficult to generate over a short period of time because of high level of genetic homogeneity of the two populations, as the F_{ST} estimates indicated. It is interesting that a similar pattern has also been found in sympatric giant pandas, another solitary bamboo-feeder. Based on the analyses of mtDNA and microsatellite, the XXL population of giant pandas was genetically differentiated with the QL and Daxiangling (DXL) populations that both are located in the north side of the Dadu River (Zhang *et al.* 2007; Zhu *et al.* 2011), whereas the LS giant panda population was not significantly differentiated with QL based on comparable mtDNA data (Zhang *et al.* 2007; Hu *et al.* 2010), also demonstrating the uniqueness of the XXL population. Accordingly, we hypothesize that historically, the XXL Mountains may experience some kind of paleoclimate or biological events (e.g., large-scaled bamboo flowering) which resulted in severe impacts on the fauna inhabiting this mountain-range including specialized bamboo-feeders (giant and red pandas). However, the histories of paleoclimate and bamboo flowering in the XXL Mountains remain unclear and in-depth study will be needed along with phylogeography researches of other sympatric species for fully understanding biogeography of this special region.

Recent population demography

Field surveys suggested a trend of population decline in red pandas (e.g., Wei *et al.* 1999); however, BOTTLENECK detected no evidence of a recent bottleneck using

both heterozygosity excess and mode-shift tests. But MSVAR simulations did detect, quantify and date the population declines for QL, XXL and GLG, supporting the conclusion of field surveys. We found that although having similar ancestral population sizes, the QL and XXL populations have smaller current effective population sizes than the GLG population. Moreover, QL and XXL appear to have undergone rapid population declines, different from a long-term contraction which GLG experienced. It is noteworthy that the estimated starting time of population declines was within the Holocene, implying less effect of the Pleistocene glaciations on these populations. Given the spatial arrangement of these populations, the differences may be explained by differential effects of recent human activities and Holocene climate fluctuations. The GLG population lives in the transition zone between the Qinghai-Tibetan Plateau and the Indo-China Peninsula where low-density human activities occur, suffering more from drastic climatic fluctuations than human activities. For example, it was estimated that the daily average temperature 300 years ago was lower by 6 °C than 1970s in this region (Yu 1996). In contrast, the QL and XXL populations are adjacent to areas of high-density human activities and are affected more by anthropogenic factors such as habitat loss, fragmentation and poaching. Historical records show that in the QL, LS and XXL mountain-ranges, average temperatures changed only 1–2 °C in the past 2000 years (Lan 1993; Zhu 2007a), suggesting less impact of climatic fluctuations on these populations. But records of human activity indicate that humans settled in the QL, LS and XXL mountain-ranges several thousands years ago and especially in the past 1000 years, human population and agriculture have rapidly expanded in these regions (Cao 2001; Zhu 2007b). Consequently, the human need for lands and resources is continuously increasing. Deforestation and poaching are found to be the two main threats driving the endangerment of red pandas, a forest-dwelling species (Glatston 1994; Wei *et al.* 1999; Choudhury 2001). For example, in Sichuan alone there were 121 forestry enterprises with over 70 000 employees at the end of 1985 (Li & Yang 1990). The scale of this industry inevitably accelerated habitat loss and fragmentation with 3597 km^2 of red panda habitat lost in the last 25 years (Li & Yang 1990). Habitat fragmentation, especially near human settlements, large roads and rivers, was also concurrent with habitat loss. Further, the demand for red pandas, and their furs and skins also threatened this species. Records showed that more than 100 skins were sold annually in the 1970s and 1980s in Tibet (Feng *et al.* 1986; Yin & Liu 1993). More than 1500 individuals have been removed from the wild by zoos and other facilities since 1953 (Wei *et al.* 1999), and 250 wild individuals in captivity were recorded in the studbook (1964–2008; Glatston 2009).

Implications for biogeography of the Qinghai-Tibetan Plateau, subspecies classification and conservation of red pandas

The Qinghai-Tibetan Plateau is well known as the highest plateau in the world and as a global biodiversity hotspot. As a medium-sized solitary mammal located on the plateau edge, red pandas demonstrated a pattern that there were no obvious phylogeographic structure and historical population expansion or contraction, suggesting historically wide gene flow and relatively stable demography, as found in other plateau edge species or populations (e.g., Hu *et al.* 2010; Qu *et al.* 2010). The findings in red pandas further corroborate the perception that species or populations along the plateau edge suffer less from the Quaternary glaciations and thus demonstrate relatively stable demography, which will contribute to a comprehensive understanding of the complex biogeography of the Qinghai-Tibetan Plateau.

Based on differences in morphology and geographical distribution, red pandas are currently classified into two subspecies: *A. f. fulgens* (Nepal, India, Butan, Myanmar, and Tibet and western Yunnan in China) and *A. f. styani* (Sichuan and Yunnan, China), and traditionally the Nujiang River was thought to be the geographical boundary of the two subspecies (Roberts & Gittleman 1984; Glatston 1994; Wei *et al.* 1999). However, this classification and the geographical boundary are debated (e.g., Groves 2011) and has remained so because of a lack of comprehensive analysis including genetic evidences. Some researchers have unsuccessfully tried to use mtDNA markers to explore subspecies differentiation (Su *et al.* 2001; Li *et al.* 2005). In this study, the identification of genetic structure based on microsatellites provided some hints on subspecies classification in this species. According to the traditional classification, the QL, LS and XXL populations belong to *A. f. styani*, the TIB population belongs to *A. f. fulgens*, and the GLG population comprises individuals of *A. f. styani* and *A. f. fulgens* from each side of the Nujiang River separately. However, STRUCTURE detected no substructure in the GLG population, suggesting that the Nujiang River may not be the geographical boundary of the two subspecies. Although our study area still did not cover the entire distribution range of red pandas, significant genetic differentiation was already detected among QL-LS, XXL and GLG-TIB. This suggested that genetic structure has occurred within or between the subspecies. Thus, the subspecies classification and their geographical boundary of the red panda need to be re-examined and future work should combine

morphological and genetic analyses of more comprehensive samples across its whole distribution range.

Phylogeography and population genetic studies can aid the identification of evolutionarily significant units and management units (Moritz 1994) and make evidence-based conservation decisions for endangered species (Szaro 2008). Our mtDNA data do not support the existence of major geographical partitions defining evolutionarily significant units; however, the microsatellite data clearly reveals three clusters: GLG-TIB, XXL and QL-LS, suggesting significant genetic differentiation and limited gene flow among clusters. Thus, these three clusters should be considered as independent management units for conservation purposes. Although red pandas harbour high genetic variations, they have suffered as a result of increased human activities. While poaching is now banned in China, the effects of habitat loss and fragmentation from historical logging, road construction and associated human activities are still ongoing. Priority should be given to the conservation and restoration of habitat, and wider international cooperation is needed for those populations that span national boundaries in Asia.

Acknowledgements

This research was supported by the National Basic Research Program of China (973 Program, 2007CB411600), the National Natural Science Foundation of China (30770399), Knowledge Innovation Program of Chinese Academy of Sciences (KSCX2-EW-Z-4) and the Royal Society. We are grateful to the following institutions for kind help in sample collection: Sichuan Forestry Department, Yunnan Forestry Department, Chongqing Zoo, Chongqing Wild Animal World and Chengdu Jintang Zoo.

References

Ahonen H, Harcourt RG, Stow AJ (2009) Nuclear and mitochondrial DNA reveals isolation of imperilled grey nurse shark populations (*Carcharias taurus*). *Molecular Ecology*, **18**, 4409–4421.

An B, Zhang LX, Browne S *et al.* (2009) Phylogeography of Tibetan snowcock (*Tetraogallus tibetanus*) in Qinghai-Tibetan Plateau. *Molecular Phylogenetics and Evolution*, **50**, 526–533.

Bandelt HJ, Forster P, Röhl A (1999) Median-joining networks for inferring intraspecific phylogenies. *Molecular Biology and Evolution*, **16**, 37–48.

Burland TG (2000) DNASTAR's Laser gene sequence analysis software. *Methods in Molecular Biology*, **132**, 71–91.

Cao SJ (2001) *The History of Chinese Population*. Publishing House of Fudan University, Shanghai, China.

Choudhury A (2001) An overview of the status and conservation of the red panda *Ailurus fulgens* in India, with reference to its global status. *Oryx*, **35**, 250–259.

Cornuet JM, Luikart G (1996) Description and power analysis of two tests for detecting recent population bottlenecks from allele frequency data. *Genetics*, **144**, 2001–2014.

Dupanloup I, Schneider S, Excoffier L (2002) A simulated annealing approach to define the genetic structure of populations. *Molecular Ecology*, **11**, 2571–2581.

Eizirik E, Kim JH, Menotti-Raymond M *et al.* (2001) Phylogeography, population history and conservation genetics of jaguars (*Panthera onca*, Mammalia, Felidae). *Molecular Ecology*, **10**, 65–79.

Evanno G, Regnaut S, Goudet J (2005) Detecting the number of clusters of individuals using the software STRUCTURE: a simulation study. *Molecular Ecology*, **14**, 2611–2620.

Excoffier L, Laval G, Schneider S (2005) Arlequin ver 3.0: an integrated software package for population genetics data analysis. *Evolutionary Bioinformatics Online*, **1**, 47–50.

Feng ZJ, Cai GQ, Zheng CL (1986) *Mammals of Tibet*. Science Press, Beijing, China.

Fu YX (1997) Statistical tests of neutrality of mutations against population growth, hitchhiking and background selection. *Genetics*, **147**, 915–925.

Glatston AR (1994) *Status Survey and Conservation Action Plan for Procyonids and Ailurids: The Red Panda, Olingos, Coatis, Raccoons, and their Relatives*. IUCN, Gland, Switzerland.

Glatston AR (2009) *International Red Panda Studbook*. Rotterdam Zoo, Rotterdam. Available from: http://www.rotterdamzoo.nl/import/assetmanager/2/6732/Red%20Panda%20Studbook.pdf.

Goossens B, Chikhi L, Ancrenaz M *et al.* (2006) Genetic signature of anthropogenic population collapse in orang-utans. *PLoS Biology*, **4**, 285–291.

Goudet J (2001) FSTAT, a program to estimate and test gene diversities and fixation indices (version 2.9.3). Updated from Goudet (1995), available from http://www.unil.ch/izea/softwares/fstat.html.

Groves C (2011) The taxonomy and phylogeny of *Ailurus*. In: *Red Panda: Biology and Conservation of the First Panda* (ed. Glatston AR). pp. 101–124, Academic Press, London.

Guindon S, Gascuel O (2003) A simple, fast, and accurate algorithm to estimate large phylogenies by maximum likelihood. *Systematic Biology*, **52**, 696–704.

Heller R, Lorenzen ED, Okello JB, Masembe C, Siegismund HR (2008) Mid-Holocene decline in African buffalos inferred from Bayesian coalescent-based analyses of microsatellites and mitochondrial DNA. *Molecular Ecology*, **17**, 4845–4858.

Hu JC (1991) Study of reproduction biology of the red panda. *Journal of Sichuan Teachers College*, **12**, 1–5.

Hu G, Du Y (2002) Current distribution, population and conservation status of *Ailurus fulgens* in Yunnan. *Journal of Northwest Forestry University*, **17**, 67–71.

Hu YB, Qi DW, Wang HJ, Wei FW (2010) Genetic evidence of recent population contraction in the southernmost population of giant pandas. *Genetica*, **138**, 1297–1306.

Kuhner MK, Yamato J, Felsenstein J (1998) Maximum likelihood estimation of population growth rates based on the coalescent. *Genetics*, **149**, 429–434.

Lan Y (1993) Preliminary study of historic climate in southwest China. *Journal of Chinese Historical Geography*, **8**, 13–39.

Li CB, Yang Y (1990) Status and assessments of forests in southern Sichuan province. In: *Forest Ecology in Sichuan* (ed. Li CB). pp. 573–586, Sichuan Science & Technology Publishing House, Chengdu, China.

Li M, Wei FW, Goossens B *et al.* (2005) Mitochondrial phylogeography and subspecific variation in the red panda

(*Ailurus fulgens*): implications for conservation. *Molecular Phylogenetics and Evolution*, **36**, 78–89.

Liang X, Zhang ZH, Zhang L *et al.* (2007) Isolation and characterization of 16 tetranucleotide microsatellite loci in the red panda (*Ailurus fulgens*). *Molecular Ecology Notes*, **7**, 1012–1014.

Librado P, Rozas J (2009) DnaSP v5: a software for comprehensive analysis of DNA polymorphism data. *Bioinformatics*, **25**, 1451–1452.

Liu ZJ, Zhang BW, Wei FW, Li M (2005) Isolation and characterization of microsatellite loci for the red panda, *Ailurus fulgens*. *Molecular Ecology Notes*, **5**, 27–29.

Liu ZJ, Ren BP, Wei FW *et al.* (2007) Phylogeography and population structure of the Yunnan snub-nosed monkey (*Rhinopithecus bieti*) inferred from mitochondrial control region DNA sequence analysis. *Molecular Ecology*, **16**, 3334–3349.

Liu ZJ, Ren BP, Wu RD *et al.* (2009) The effect of landscape features on population genetic structure in Yunnan snub-nosed monkeys (*Rhinopithecus bieti*) implies an anthropogenic genetic discontinuity. *Molecular Ecology*, **18**, 3831–3846.

Luikart G, Allendorf FW, Cornuet JM, Sherwin WB (1998) Distortion of allele frequency distributions provides a test for recent population bottlenecks. *Journal of Heredity*, **89**, 238–247.

Mantel N (1967) The detection of disease clustering and a generalized regression approach. *Cancer Research*, **27**, 209–220.

Moritz C (1994) Application of mitochondrial DNA analysis in conservation: a critical review. *Molecular Ecology*, **3**, 401–411.

Myers N, Mittermeier RA, Mittermeier CG *et al.* (2000) Biodiversity hotspots for conservation priorities. *Nature*, **403**, 853–858.

Nei M (1987) *Molecular Evolutionary Genetics*. Columbia University Press, New York.

Paetkau D, Amstrup SC, Born EW *et al.* (1999) Genetic structure of the world's polar bear populations. *Molecular Ecology*, **8**, 1571–1584.

Piry S, Luikart G, Cornuet JM (1999) Bottleneck: a computer program for detecting recent reductions in the effective population size using allele frequency data. *Journal of Heredity*, **90**, 502–503.

Posada D (2008) jModelTest: phylogenetic model averaging. *Molecular Biology and Evolution*, **25**, 1253–1256.

Princée FPG (1989) Preservation of genetic variation in the red panda population. In: *Red Panda Biology* (ed Glatston AR). pp. 171–182, SPB Academic Publishing, The Hague, The Netherlands.

Pritchard JK, Stephens M, Donnelly P (2000) Inference of population structure using multilocus genotype data. *Genetics*, **155**, 945–959.

Qu YH, Lei FM (2009) Comparative phylogeography of two endemic birds of the Tibetan plateau, the white-rumped snow finch (*Onychostruthus taczanowskii*) and the Hume's ground tit (*Pseudopodoces humilis*). *Molecular Phylogenetics and Evolution*, **51**, 312–326.

Qu YH, Lei FM, Zhang RY, Lu X (2010) Comparative phylogeography of five avian species: implications for Pleistocene evolutionary history in the Qinghai-Tibetan plateau. *Molecular Ecology*, **19**, 338–351.

Ramos-Onsins SE, Rozas J (2002) Statistical properties of new neutrality tests against population growth. *Molecular Biology and Evolution*, **19**, 2092–2100.

Rice WR (1989) Analyzing tables of statistical tests. *Evolution*, **43**, 223–225.

Roberts MS, Gittleman JL (1984) *Ailurus fulgens*. *Mammalian Species*, **222**, 1–8.

Rousset F (2008) GENEPOP'007: a complete re-implementation of the GENEPOP software for Windows and Linux. *Molecular Ecology Resources*, **8**, 103–106.

Sakka H, Quéré JP, Kartavtseva I *et al.* (2010) Comparative phylogeography of four *Apodemus* species (Mammalia: Rodentia) in the Asian Far East: evidence of Quaternary climatic changes in their genetic structure. *Biological Journal of the Linnean Society*, **100**, 797–821.

Sambrook J, Fritsch EF, Maniatis T (1989) *Molecular Cloning: A Laboratory Manual*, 2nd edn. Cold Spring Harbor Press, Cold Spring Harbor Laboratory, Cold Spring Harbor.

Shriver MD, Jin L, Chakraborty R, Boerwinkle E (1993) VNTR allele frequency distributions under the stepwise mutation model: a computer-simulation approach. *Genetics*, **134**, 983–993.

Storz JF, Beaumont MA (2002) Testing for genetic evidence of population expansion and contraction: an empirical analysis of microsatellite DNA variation using a hierarchical Bayesian model. *Evolution*, **56**, 154–166.

Su B, Fu YX, Wang YX, Jin L, Chakraborty R (2001) Genetic diversity and population history of the red panda (*Ailurus fulgens*) as inferred from mitochondrial DNA sequence variations. *Molecular Biology and Evolution*, **18**, 1070–1076.

Swofford DL (2002) *PAUP: Phylogenetic Analysis Using Parsimony (and Other Methods) 4.0 Beta*. Sinauer Associates, Sunderland, MA.

Szaro RC (2008) Endangered species and nature conservation: science issues and challenges. *Integrative Zoology*, **3**, 75–82.

Taberlet P, Griffin S, Goossens B *et al.* (1996) Reliable genotyping of samples with very low DNA quantities using PCR. *Nucleic Acids Research*, **24**, 3189–3194.

Tajima F (1983) Evolutionary relationship of DNA sequences in finite populations. *Genetics*, **105**, 437–460.

Tajima F (1989) Statistical method for testing the neutral mutation hypothesis by DNA polymorphism. *Genetics*, **123**, 585–595.

Tamura K, Dudley J, Nei M, Kumar S (2007) MEGA4: Molecular Evolutionary Genetics Analysis (MEGA) software version 4.0. *Molecular Biology and Evolution*, **24**, 1596–1599.

Urquhart J, Wang Y, Fu J (2009) Historical vicariance and male-mediated gene flow in the toad-headed lizards *Phrynocephalus przewalskii*. *Molecular Ecology*, **18**, 3714–3729.

Van Loon EE, Cleary DFR, Fauvelot C (2007) ARES: software to compare allelic richness between uneven samples. *Molecular Ecology Notes*, **7**, 579–582.

Van Oosterhout C, Hutchinson WF, Wills DPM, Shipley P (2004) MICRO-CHECKER: software for identifying and correcting genotyping errors in microsatellite data. *Molecular Ecology Notes*, **4**, 535–538.

Walsh PS, Metzger DA, Higuchi R (1991) Chelex 100 as a medium for simple extraction of DNA for PCR-based typing from forensic material. *BioTechniques*, **10**, 506–513.

Watterson GA (1975) On the number of segregating sites. *Theoretical Population Biology*, **7**, 256–276.

Wei FW, Feng ZJ, Wang ZW, Hu JC (1999) Current distribution, status and conservation of wild red pandas *Ailurus fulgens* in China. *Biological Conservation*, **89**, 285–291.

Wilson GA, Rannala B (2003) Bayesian inference of recent migration rates using multilocus genotypes. *Genetics*, **163**, 1177–1191.

Xia X, Xie Z (2001) DAMBE: software package for data analysis in molecular biology and evolution. *Journal of Heredity*, **92**, 371–373.

Yin BG, Liu WL (1993) *Precious and Rare Wildlife and its Protection in Tibet*. China Forestry Publishing House, Beijing, China.

Yu XX (1996) The snow in the Cang Mountains and historical climatic changes in Yunnan. *Journal of Chinese Historical Geography*, **11**, 25–39.

Zhan XJ, Li M, Zhang ZJ *et al.* (2006) Molecular censusing doubles giant panda population estimate in a key nature reserve. *Current Biology*, **16**, R451–R452.

Zhan XJ, Zheng XD, Bruford MW, Wei FW, Tao Y (2010) A new method for quantifying genotyping errors for noninvasive genetic studies. *Conservation Genetics*, **11**, 1567–1571.

Zhang FF, Jiang ZG (2006) Mitochondrial phylogeography and genetic diversity of Tibetan gazelle (*Procapra picticaudata*): implications for conservation. *Molecular Phylogenetics and Evolution*, **41**, 313–321.

Zhang BW, Li M, Ma LC, Wei FW (2006) A widely applicable protocol for DNA isolation from fecal samples. *Biochemical Genetics*, **44**, 503–512.

Zhang BW, Li M, Zhang ZJ *et al.* (2007) Genetic viability and population history of the giant panda, putting an end to the ''evolutionary dead end''? *Molecular Biology and Evolution*, **24**, 1801–1810.

Zhu SZ (2007a) Climate changes in Liangshan Mountain areas since 10000 years before. *Yunnan Geographic Environment Research*, **19**, 1–4.

Zhu SZ (2007b) Historic forest changes of the Liangshan Mountains in Sichuan Province. *Journal of Chinese Historical Geography*, **22**, 43–52.

Zhu LF, Zhang SN, Gu XD, Wei FW (2011) Significant genetic boundaries and spatial dynamics of giant pandas occupying fragmented habitat across southwest China. *Molecular Ecology*, **20**, 1122–1132.

F.W.W. leads a research group of animal ecology and conservation genetics at the Institute of Zoology, Chinese Academy of Sciences, and focuses on ecology and conservation genetics of endangered mammals in China. Y.B.H., Y.G., D.W.Q., X.J.Z. and H.W. are members of Wei's research group and are interested in animal molecular ecology and landscape ecology. M.W.B. is interested in population biology and genetics of endangered species.

Data Accessibility

DNA sequences: GenBank accession nos HQ992964–HQ992985.

Final DNA sequence assembly: uploaded as online supporting material.

Population microsatellite data: DRYAD entry doi: 10.5061/dryad.9096.

Supporting information

Additional supporting information may be found in the online version of this article.

Table S1 Information of red panda samples used in this study.

Table S2 Information of nine microsatellite loci used in this study, including label type, allele size and number of alleles (*A*) found in each locus.

Table S3 Variable nucleotide sites of mtDNA control region haplotypes in this study. Dots (.) indicate identical nucleotides.

Table S4 Distribution of mtDNA control region haplotypes among five red panda populations.

Table S5 Medians of current (N_0) and ancestral effective population sizes (N_1) and time since population decline (T) for the QL, XXL and GLG populations based on a generation time of 2 or 6 years, using Bayesian MSVAR simulations.

Fig. S1 Comparison of allelic richness (the number of alleles) among four populations of red pandas. Allelic richness was estimated from nine-locus combined genotypes and extrapolated beyond the sample sizes using ARES.

Fig. S2 Unrooted maximum-likelihood (ML) tree based on HKY distances among mtDNA CR haplotypes of red pandas. Bootstrap values are given next to nodes based on 1000 bootstrap simulations.

Please note: Wiley-Blackwell are not responsible for the content or functionality of any supporting information supplied by the authors. Any queries (other than missing material) should be directed to the corresponding author for the article.